Hot-electron noise in two-valley semiconductors: An analytic model

Christopher J. Stanton,* and John W. Wilkins
Laboratory of Atomic and Solid State Physics, Cornell University, Ithaca, New York 14853
and Institute for Theoretical Physics, University of California, Santa Barbara, California 93106
(Received 18 August 1986)

We present results for the hot-electron noise in two-valley semiconductors, such as GaAs, where intervalley transfer plays an important role. The noise is calculated by a Boltzmann–Green-function method. We obtain an analytic solution for a model with two valleys and three relaxation times. Using the measured low-field mobility, lower-valley mass, and valley separation energy Δ, while adjusting three upper-valley parameters, we obtain good agreement with both experimental time-of-flight measurements and microwave noise measurements. We find that the hot-electron noise is very sensitive to the transport parameters, much more so than the velocity-field curve. In particular, the noise is very sensitive to the Γ-to-L scattering rate and our results indicate that experimental noise measurements might be used for determining this parameter.

I. INTRODUCTION

Hot-electron noise (i.e., nonequilibrium current fluctuations) in semiconductors is of great interest from both a fundamental and applied point of view. From a fundamental viewpoint, nonequilibrium noise can provide additional information about a system that is not available from the I-V curve. This is not true in equilibrium where the fluctuation-dissipation theorem requires that the noise be proportional to the conductivity. Furthermore, as we shall see, the nonequilibrium noise can be more sensitive to the various scattering rates and transport parameters than the conductivity, and can be used to deduce these parameters. From an applied viewpoint, many of the devices in use today operate in the high-electric-field regime, and thus a knowledge of hot-electron noise is essential to the design and performance of these devices.

In this paper, we calculate the hot-electron noise in bulk GaAs. The noise is interesting not only because of the heating effects in the lower Γ valley due to the strong electric fields, but also because of the fluctuations associated with the transfer of the electrons between the Γ and L valleys (intervalley noise).

Previous calculations of the hot-electron noise in GaAs have either been Monte Carlo calculations[1–4] or have assumed[5,6] that the distribution functions were displaced Maxwellians so that a generalized Einstein relation holds, i.e., the noise is proportional to the electron temperature times a differential mobility. Prior calculations in GaAs (Refs. 7–9) show that the distribution function in the Γ valley is clearly not Maxwellian, and thus the validity of a generalized Einstein relation is questionable. Here, we use a Boltzmann–Green-function method to obtain an analytic expression for the current noise. The method is based on finding the time evolution of the velocity of a single electron given by the time-dependent Boltzmann equation. The method is valid for nondegenerate semiconductors when electron-electron scattering is not important. The results obtained are in fair agreement with the time-of-flight data of Ruch and Kino[10] and the microwave noise measurements of Gasquett[11] *et al.* and Bareikis *et al.*[12] We find that the nonequilibrium noise is fairly sensitive to the transport parameters that enter in the model, more so than the velocity-field curve. In particular, we find that the noise is extremely sensitive to the Γ-to-L scattering rate, suggesting that noise measurements might be used to determine this rate.

II. THE MODEL

The important features of the band structure of GaAs are the minimum in the conduction band at the Γ point and the satellite minima at the L points separated from the Γ-valley minimum by an energy $\Delta \approx 0.3$ eV. The spherical Γ valley has a mass of $0.069m_e$. The L valleys are ellipsoidal, and the masses are not known extremely well, although the density-of-states mass in the L valley has been estimated to be about $m_L^* \approx 0.2m_e - 0.5m_e$.[13,14]

We model the dynamics of the system with parabolic Γ and L valleys and a coupled set of Boltzmann equations, one for the Γ valley and one for a single, generic L valley. A distribution function, $f_\Gamma(v)$ or $f_L(v)$, normalized to the density of electrons, n_Γ or n_L, describes the electrons in each valley. The collision integral in the Boltzmann equation is approximated by a relaxation-to-local-equilibrium form for both the intravalley and intervalley processes. The collision integrals are chosen so that particle number is conserved in the collision process. Details of the approximation of the collision integrals to relaxation-time form are given in Refs. 7, 15, and 16. Finally, we neglect electron motion perpendicular to the electric field; our model is one dimensional in velocity. The resulting coupled Boltzmann equations are

$$\frac{\partial f_\Gamma}{\partial t} + \frac{eE}{m_\Gamma^*}\frac{\partial f_\Gamma}{\partial v} = -\frac{1}{\tau_{\Gamma\Gamma}}[f_\Gamma(v) - f_{\Gamma,\mathrm{LE}}(v)] - \frac{\Theta(v^2 - v_c^2)}{\tau_{\Gamma L}}\left[f_\Gamma(v) - \frac{n_\Gamma^0 n_L}{n_L^0 n_\Gamma} f_{\Gamma,\mathrm{LE}}(v)\right], \tag{1a}$$

$$\frac{\partial f_L}{\partial t}+\frac{eE}{m_L^*}\frac{\partial f_L}{\partial v}=-\frac{1}{\tau_{LL}}[f_L(v)-f_{L,\mathrm{LE}}(v)] -\frac{1}{\tau_{L\Gamma}}\left[f_L(v)-\frac{n_\Gamma^{>}n_L^0}{n_\Gamma^{0,>}n_L}f_{L,\mathrm{LE}}(v)\right] . \tag{1b}$$

Here, m_Γ^* and m_L^* are the effective masses, and n_L^0 and n_Γ^0 are the equilibrium valley densities which are determined by the density of states. For parabolic bands in d dimensions with an L-valley degeneracy N,

$$n_\Gamma^0=n_{\mathrm{tot}}\frac{1}{1+N\exp\left[\frac{-\Delta}{k_BT_0}\right]\left[\left[\frac{m_L^*}{m_\Gamma^*}\right]^{1/2}\right]^d} , \qquad n_L^0=n_{\mathrm{tot}}\frac{N\exp\left[\frac{-\Delta}{k_BT_0}\right]\left[\left[\frac{m_L^*}{m_\Gamma^*}\right]^{1/2}\right]^d}{1+N\exp\left[\frac{-\Delta}{k_BT_0}\right]\left[\left[\frac{m_L^*}{m_\Gamma^*}\right]^{1/2}\right]^d} , \tag{2}$$

so that in one dimension with an L-valley degeneracy of one, the ratio of the valley populations is

$$\frac{n_\Gamma^0}{n_L^0}=\left[\frac{m_\Gamma^*}{m_L^*}\right]^{1/2}\exp\left[\frac{\Delta}{k_BT_0}\right] . \tag{3}$$

The local-equilibrium functions, $f_{\Gamma,\mathrm{LE}}(v)$ and $f_{L,\mathrm{LE}}(v)$ are Maxwellians with the mass of the respective valley, normalized to the density of f_Γ and f_L,

$$f_{\Gamma,\mathrm{LE}}(v)=\frac{n_\Gamma}{n_\Gamma^0}f_{\Gamma,\mathrm{eq}}(v) , \qquad f_{L,\mathrm{LE}}(v)=\frac{n_L}{n_L^0}f_{L,\mathrm{eq}}(v) . \tag{4}$$

Finally $n_\Gamma^{>}$, and $n_\Gamma^{0,>}$ are the number of electrons in the Γ valley with energy greater than Δ, i.e.,

$$\left.\begin{matrix} n_\Gamma^{>} \\ n_\Gamma^{0,>}\end{matrix}\right\}=\int_{v^2>v_c^2}dv\times\begin{cases}f_\Gamma(v)\\ f_{\Gamma,\mathrm{eq}}(v)\end{cases} . \tag{5}$$

Again, the superscript zero denotes an equilibrium density.

The first term on the right-hand side of Eq. (1a) is the collision integral for Γ-to-Γ scattering. The second term represents Γ-to-L scattering. The Θ function in the Γ-to-L term permits only those particles with energy greater than Δ to transfer from the Γ to the L valley. In the actual system, electrons can transfer from the Γ valley to the L valley when they are within an optic-phonon energy of the L-valley minimum. Since the optic-phonon energy for GaAs, 35 meV, is small compared to $\Delta\approx 0.3$ eV, our approximation is reasonable. The first term on the right-hand side of the second equation is the collision integral for L-to-L scattering. The second term is the Γ-to-Γ scattering term. The coefficients of the local equilibrium functions in the intervalley scattering terms are nonuniquely determined by the requirements of particle and current conservation.

III. STEADY-STATE PROPERTIES

There is a straightforward (if tedious) procedure for solving the coupled set of equations. The two equations are coupled only through the densities; n_L appears in the equation for f_Γ and $n_\Gamma^{>}$ appears in the equation for f_L. Once the densities are known, the equations uncouple and the distribution functions can be found by using integrating factors to directly integrate the equations. To find the densities, Eq. (1a) is solved to determine f_Γ in terms of n_Γ and n_L. We then integrate f_Γ over velocity to obtain n_Γ as a functional of n_Γ and n_L. Using the constraint $n_\Gamma+n_L=n_{\mathrm{tot}}$, we are left with an algebraic equation for n_Γ which is easily solved. The steady-state solution of the model for the velocity-field curves and the distribution functions has been published[7] previously (note in that solution the electron is assumed to have a charge $-e$, whereas in this paper we assume for convenience that the electron has a charge $+e$). The v-E curve obtained there agreed fairly well with the experimental data, and the distribution function in the Γ valley deviated substantially from Maxwellian, showing structure at the valley separation energy.

IV. NOISE PROPERTIES

To calculate the noise in the two-valley model, we make use of the Boltzmann–Green-function method described in earlier papers.[17,18] The method involves three steps. First, the steady-state distribution function is calculated from the time-independent Boltzmann equation. Next, the Green function or response function $R(v,t\mid v_0)$ is calculated from the time-dependent Boltzmann equation, subject to the initial condition that at time $t=0$, the electron has velocity v_0. Finally the current correlation function is calculated from the expression

$$\Gamma(t)=\left[\frac{e}{2l}\right]^2\int_{-\infty}^{\infty}\int_{-\infty}^{\infty}dv\,dv_0vv_0R(v,t\mid v_0)f(v_0) , \tag{6}$$

where $2l$ is the length of the system. The noise power spectrum is just twice the cosine transform of the current correlation function.

Calculating the noise for the two-valley model is complicated by the necessity to compute four Green functions corresponding to the response of the Γ valley to an electron initially in the Γ valley, the response of the L valley to an electron initially in the Γ valley, etc. This leads to four power spectra, $S_{\Gamma,\Gamma}$, $S_{L,L}$, $S_{\Gamma,L}$, and $S_{L,\Gamma}$. The details of the calculation are outlined in the Appendix. Only the $\omega\rightarrow 0$ limit of the noise is calculated; not only is calculating the full frequency dependence difficult but also the frequency dependence is apt to be excessively sensitive to the approximations made for the collision integrals.

The results for the noise are shown in Fig. 1. The solid line is the calculated noise from our model. The squares are the experimental data of Ruch and Kino[10] calculated from time-of-flight measurements of the diffusion constant. The error bars are 20%, which is the quoted error in the paper. The solid circles are from the experimental data of Bareĭkis *et al.*[12] and the open circles are from the experimental data of Gasquet *et al.*[11] These data points were determined by microwave noise measurements.

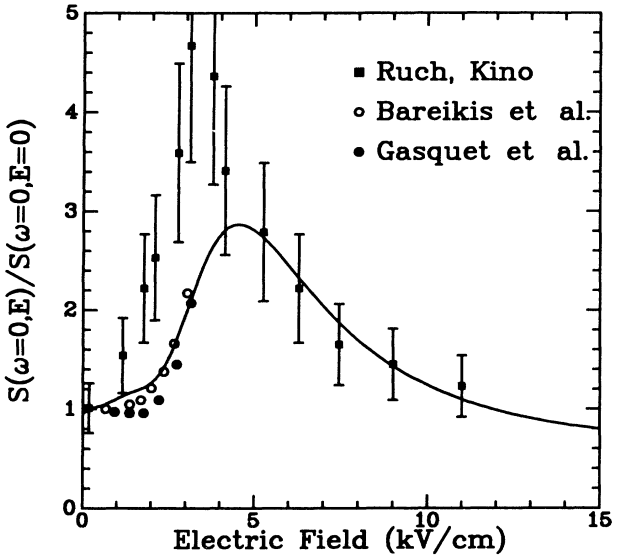

FIG. 1. The noise for the two-valley model of GaAs compared with the experimental data. The solid line is the calculated curve using the following values for the parameters: $\mu_{\Gamma\Gamma}=7500$ cm^2/V sec, $m_\Gamma^*=0.067m_e$, $m_L^*=1.2m_e$, $\tau_{\Gamma L}^{-1}/\tau_{\Gamma\Gamma}^{-1}=3.5$, and $\tau_{LL}^{-1}/\tau_{\Gamma\Gamma}^{-1}=10$. The squares are from the experimental data of Ruch and Kino (Ref. 10) and the error bars are 20% (the quoted value). Ruch and Kino's data is from a time-of-flight measurement of the diffusion constant. The solid circles are from the data of Gasquet *et al.* (Ref. 11) and the open circles are from the data of Bareĭkis *et al.* (Ref. 12). Gasquet and Bareĭkis's data are from microwave noise measurements.

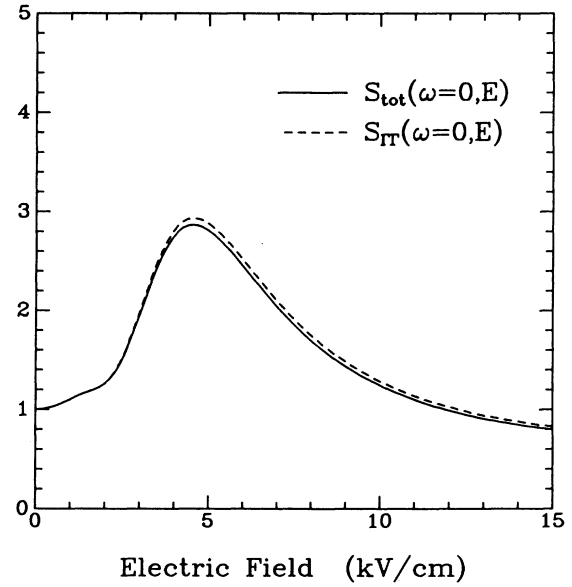

FIG. 2. The $S_{\Gamma,\Gamma}$ contribution to the noise compared with the total contribution. The total noise is dominated by the $S_{\Gamma,\Gamma}$ term. This is due to the fact that the mass and the scattering rate in the Γ valley are much smaller than these quantities in the L valley.

There is a disagreement between the time-of-flight and the noise data at low electric field. One possible explanation for this discrepancy has been suggested by Glisson *et al.*[3] They showed, using Monte Carlo simulations, that circuit effects such as contact resistance and oscilloscope rise time could lead to a diffusion constant, as determined by the time-of-flight technique, that was larger than the actual diffusion constant especially in the region of intervalley transfer. In view of the differences between the three sets of experimental data, it appears this is the case.

Many aspects of the noise results can be simply understood notwithstanding the complicated details of the calculations. Figure 2 shows that $S_{\Gamma,\Gamma}$ term completely dominates the noise. This is not unexpected since, in equilibrium, the noise scales with τ/m^*. Since the upper valley has both a larger mass (factor of 17) and a larger scattering rate (factor of 10) than the lower valley, we would expect that any component of the noise involving the upper valley would be much smaller than $S_{\Gamma,\Gamma}$.

Figure 3 displays the various contributions to $S_{\Gamma,\Gamma}$. The expressions for the components are given in the Appendix after Eq. (A28). The solid line is the thermal equilibrium noise. At high fields, the number of electrons in the Γ valley is reduced and this component decreases. The short-dashed line results from the heating of the Γ-valley distribution by the electric field. In a single-valley model, this term would increase quadratically with the electric field (for a constant scattering time). For two val-

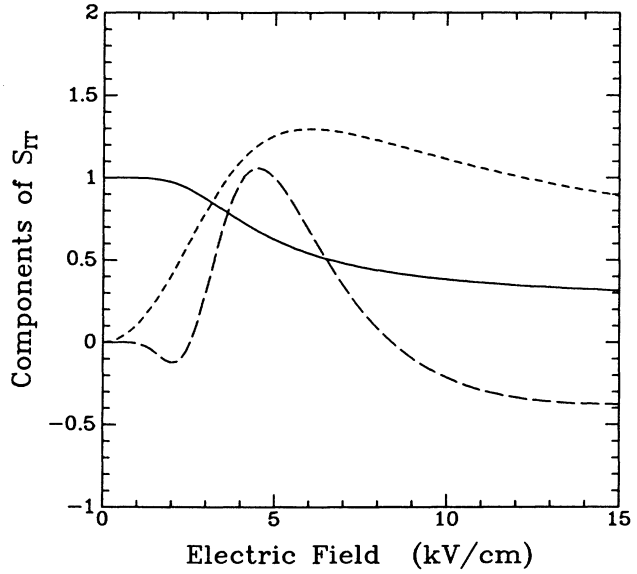

FIG. 3. The components of $S_{\Gamma,\Gamma}$. The solid line is the thermal equilibrium noise contribution. It decreases because the number of carriers in the Γ valley decreases as a function of the electric field. The short-dashed line is the heating component that is due to the increase in electron temperature in the Γ valley as the electric field increases. This contribution also decreases at high fields because of the reduction in the number of Γ-valley electrons. The long-dashed line represents the contribution to the noise that arises because the electrons fluctuate between the Γ and L valleys. The expressions for these components are given after Eq. (A28) in the Appendix.

leys, this component must decrease at very large fields simply because the number of electrons in the Γ valley decreases. The last term (long-dashed line) is not present in a single-valley model. It arises from the scattering of an electron out of the Γ valley into the L valley and then eventually back into the Γ valley. This term has a maximum for electric fields where the differential mobility is negative and the slope of the number of electrons in the Γ-valley versus electric field curve is large. For high electric fields this term is negative. This occurs since most electrons initially scatter out of the Γ valley with positive velocity. They scatter back from the L valley isotropically into the Γ valley. Those electrons that scatter back with negative velocity are then accelerated by the electric field and cannot scatter back into the L valley, whereas the electrons that scatter back with positive velocities, even when accelerated by the field, can still scatter back into the L valley. This leads to a negative correlation at high fields.

A. Sensitivity to parameters

Figures 4 and 5 display the sensitivity of the v-E curve and the noise spectrum, respectively, to four important parameters: (i) the valley separation Δ, (ii) the mass of the upper valley m_L^*, (iii) the ratio of the Γ-to-L scattering rate compared to the intravalley scattering rate $\tau_{\Gamma L}^{-1}/\tau_{\Gamma\Gamma}^{-1}$, and (iv) the ratio of the intravalley scattering rates $\tau_{LL}^{-1}/\tau_{\Gamma\Gamma}^{-1}$. Comparing the two figures, the overall conclusion is that the v-E curve is relatively insensitive to all the parameters, in contrast to the noise spectrum which is exceedingly sensitive to parameters (i) and (iii)—namely, the valley separation and the Γ-to-L scattering rate. Since the valley separation is relatively well known, we stress that the measurement of the noise spectra could be a good way to determine the intervalley scattering rates.

Below we analyze the sensitivity of the v-E curve and the noise spectrum to the four parameters listed in the previous paragraph.

(i) *Valley separation energy* Δ. As the valley separation energy increases, the Γ-valley electrons need a higher energy to transfer into the L valley and thus the number of Γ electrons increases. Given the lower mass and lower scattering rate of the Γ valley, a larger Δ must increase both the maximum velocity and the electric field at which the maximum velocity occurs (cf. Fig. 3). Since there are more electrons in the Γ valley, the noise spectrum also increases from both the heating and intervalley fluctuation components of $S_{\Gamma,\Gamma}$ (cf. short-dashed and long-dashed lines in Fig. 3).

(ii) *Upper-valley mass* m_L^*. The mass effects of the v-E curve through the density of states $[\propto (m_L^*)^{1/2}]$ and the mobility of the L valley. An increase in m_L^* will, through both of these effects, cause the average velocity to decrease. The effect of m_L^* on the noise is more subtle. As mentioned, increasing the mass increases the population of the L valley through the density of states. This causes the heating component in Fig. 3 (short-dashed line) to decrease (since the number of electrons in the Γ valley is decreased). At intermediate fields, however, the intervalley fluctuation component (cf. long-dashed line in Fig. 3) increases enough to lead to an overall increase in the noise. At high fields, where the intervalley fluctuation term is small, the decrease in the heating component dominates and the noise decreases with increasing mass.

(iii) Γ-*to-L scattering rate* $\tau_{\Gamma L}^{-1}$. The dependence of the v-E curve on the intervalley scattering rate is fairly complicated. At intermediate fields (in the negative differential mobility regime) a large intervalley scattering decreases the fraction of electrons in lower valley with energies greater than Δ, and therefore decreases the number of electrons in the L valley; hence there are more electrons in the higher-mobility Γ valley and the average velocity increases. At large fields, even though there are only a few Γ-valley electrons, they still dominate the average velocity since their mobility is high. Increasing

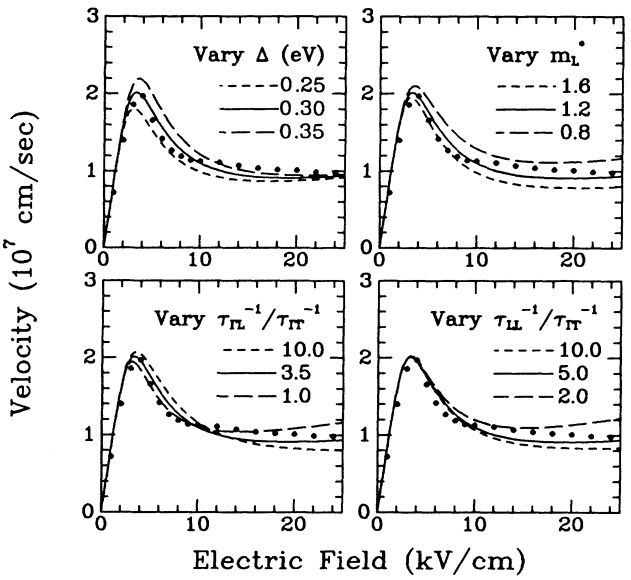

FIG. 4. The sensitivity of the velocity-field curve to the various parameters that enter the model. These figures are based on results of Baranger (Ref. 16). In all figures, the solid line is the best fit and the dots are the compiled experimental data. The upper-left-hand figure shows the sensitivity to the valley separation energy Δ. As Δ increases, the Γ-valley electrons need to reach a higher energy before they can transfer into the L valley, and thus the maximum velocity occurs for a higher electric field and is larger as Δ increases. The upper-right-hand figure shows the sensitivity to the upper-valley mass. The mass effects the v-E curve through the density of states in the L valley $[\propto (m_L^*)^{1/2}]$ and the mobility of the upper valley. An increase in m_L^* will, through both of these effects, cause the average velocity to decrease. The lower-left-hand figure shows the sensitivity to the Γ-to-L scattering rate. At intermediate fields, as the rate increases, the number of electrons in the Γ valley below the energy threshold Δ increases and thus the peak in the v-E curve is higher and occurs at a greater electric field. At higher fields, even though there are only a few electrons in the Γ valley, they still have a large effect on the average velocity since their mobility is high. An increase in $\tau_{\Gamma L}^{-1}$ causes a decrease in the Γ-valley mobility and the average velocity. The lower-right-hand figure shows the sensitivity to the L intervalley scattering rate. As τ_{LL}^{-1} increases, the mobility of the electrons in the L valley decreases and thus the v-E curve at high fields decreases.

$\tau_{\Gamma L}^{-1}/\tau_{\Gamma\Gamma}^{-1}$ thus decreases the average velocity. For the noise spectrum, we note that it is very sensitive to this scattering rate; in particular the intervalley fluctuation component [cf. last term of (A28) and the above discussion of Fig. 3]. A decreasing $\tau_{\Gamma L}^{-1}/\tau_{\Gamma\Gamma}^{-1}$ increases the correlation time for the intervalley scattering and therefore increases this component.

(iv) *Ratio of the intravalley scattering rates* $\tau_{LL}^{-1}/\tau_{\Gamma\Gamma}^{-1}$. The v-E curve has only a slight dependence on $\tau_{LL}^{-1}/\tau_{\Gamma\Gamma}^{-1}$. This is at high electric fields where the average velocity is dominated by the L-valley electrons. As τ_{LL}^{-1} increases, the mobility of the L-valley electrons decreases, causing the average velocity to decrease. The noise is not very sensitive to τ_{LL}^{-1} since the L-to-L scattering rate primarily affects $S_{L,L}$, which is much smaller than $S_{\Gamma,\Gamma}$ (cf. Fig. 2).

V. DISCUSSION

Because the noise is so sensitive to the Γ-to-L scattering rate, it might be used to determine the rate. Figure 6 shows two fits of the parameters for the v-E curve and the noise. Fit 1 has the parameters $\Delta=0.3$ eV, $m_L^*=1.2m_e$, $\tau_{\Gamma L}^{-1}/\tau_{\Gamma\Gamma}^{-1}=3.5$, and $\tau_{LL}^{-1}/\tau_{\Gamma\Gamma}^{-1}=5.0$ while fit 2 has the parameters $\Delta=0.35$ eV, $m_L^*=1.8m_e$, $\tau_{\Gamma\Gamma}/\tau_{\Gamma L}=0.5$, and $\tau_{\Gamma\Gamma}/\tau_{LL}=15.0$. As can be seen, the resulting v-E curves are very similar and agree reasonably well with the experimental data. The noise curves, however, are extremely different, and only fit 1 is close to the experimental data. This is because fit 2 has a very small value for the Γ-to-L scattering rate and the noise is very sensitive to this parameter, while the v-E curve is not. Note the parameters of the fit are similar to those used to generate Fig. 1.

We believe that our model resolves the discrepancy between experimental data for the diffusion constant and theoretical attempts to explain it. As pointed out by Glisson *et al.*,[3] if Monte Carlo calculations of the diffusion coefficient versus electric field are brought into agreement with experimental data, then agreement is sacrificed in the velocity-field curve or low-field mobility. As mentioned earlier, part of this discrepancy was shown by Glisson *et al.*[3] to be due to circuit effects. By allowing for circuit effects, they brought into agreement the experimental and Monte Carlo results for the diffusion constant at low field (<6 kV/cm). However, their Monte Carlo results were still too low at high fields (>6 kV/cm) and this could not be accounted for by circuit effects.

Our model, though overly simplistic (we have neglected valley nonparabolicity as well as scattering to the X valley) shows that by slightly decreasing the $\Gamma\rightarrow L$ scattering, the value of the diffusion coefficient at high fields (>6 kV/cm) can be increased without substantially changing the velocity-field curve (cf. Figs. 4 and 5).

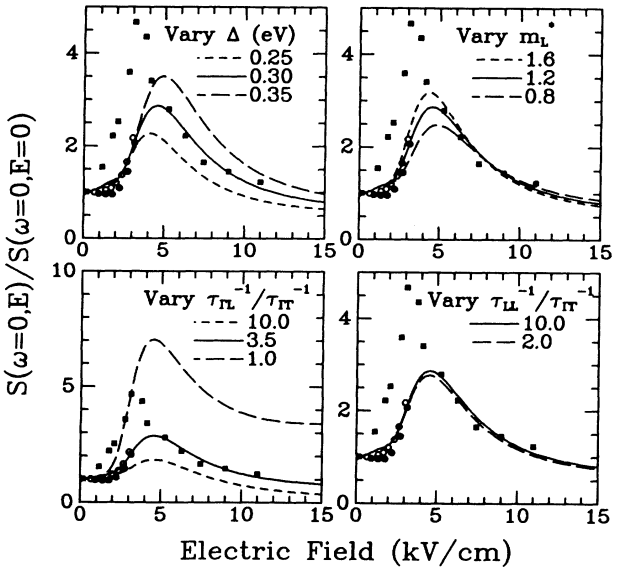

FIG. 5. The sensitivity of the noise to the transport parameters. The upper-left-hand figure shows the sensitivity to Δ. As Δ decreases, transfer to the upper valley occurs at a lower field and the noise decreases due to the fact that electrons in the Γ valley do not heat up but transfer to the L valley instead. The upper-right-hand figure shows the sensitivity to m_L^*. The density of states in the L valley increases $\propto(m_L^*)^{1/2}$ which causes the intervalley noise to increase with the upper-valley mass. The lower-left-hand figure shows the sensitivity to the Γ-to-L scattering rate. As can be seen, the noise is extremely sensitive to this parameter. From Fig. 3, we see that the noise in the negative differential mobility region is sensitive to the fluctuations in the number of carriers in the Γ valley. As the Γ-to-L scattering rate increases, the correlation time for these fluctuations decreases and the noise decreases at all values of the electric field. The last figure shows the sensitivity of the noise to the L-to-L scattering rate. The noise is not very sensitive to this quantity (the L-to-L scattering rate will have more of an effect on the $S_{L,L}$ term, but since this term is smaller than the $S_{\Gamma,\Gamma}$ term, the L-to-L rate does not have a large effect on the total noise).

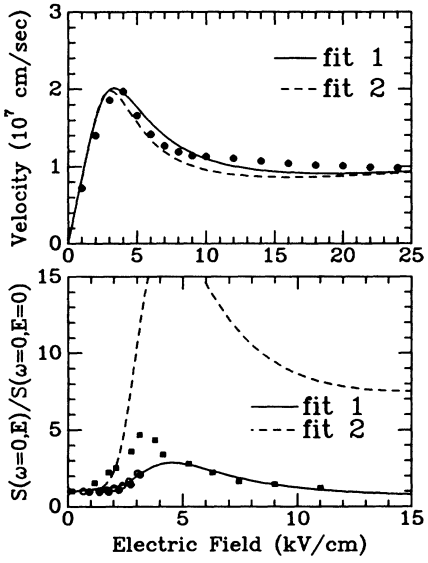

FIG. 6. Two fits for the v-E curve and noise. While the fits for the v-E are very close to the experimental data, the fits for the noise differ considerably. This is because the noise is extremely sensitive to the value of the Γ-to-L scattering rate while the average velocity is not. This suggests that noise measurements could be used to determine some of the unknown transport parameters in many-valley semiconductors.

VI. CONCLUSIONS

To summarize the results of this paper, we have proposed a simple model for transport in many-valley semiconductors such as GaAs which includes coupling between the central Γ valley and the satellite L valleys. The coupled equations are chosen so that certain properties of the collision integrals are obeyed (e.g., particle conservation, relaxation to local equilibrium, etc.). The model treats the scattering rates and band structure simplistically but has the advantage that it is analytically solvable for both the velocity-field curve and the noise. The model predicts that the noise should be very sensitive to the Γ-to-L scattering rate while the v-E curve should not be that sensitive, and suggests that noise measurements might be useful in determining some of the transport parameters.

ACKNOWLEDGMENTS

The work on developing the model and the solution for the steady-state distribution function and velocity-field curves was done in collaboration with Harold Baranger, to whom we are grateful. This work was supported by the U.S. Office of Naval Research and by the Semiconductor Research Corporation. One of us (C.J.S.) gratefully acknowledges the support of the Fannie and John Hertz Foundation. The work at the Institute for Theoretical Physics was supported in part by the National Science Foundation supplemented by funds from the National Aeronautics and Space Administration.

APPENDIX A: SOME DETAILS OF THE CALCULATION FOR THE NOISE

In this appendix, we outline the steps of the calculation of the noise in the two-valley model of GaAs discussed in Sec. IV. The procedure is very similar to that for calculating the steady-state behavior.

The starting point is the time-dependent coupled Boltzmann equations for the Green functions. There are four Green functions, which are denoted by $R_{\Gamma,\Gamma}(v,t \mid v_0)$, $R_{\Gamma,L}(v,t \mid v_0)$, $R_{L,L}(v,t \mid v_0)$, and $R_{L,\Gamma}(v,t \mid v_0)$ where the second subscript denotes the valley the electron was in at time $t=0$ and the first subscript denotes the valley that the electron was in at time t. The coupled equations for the Green functions are

$$\begin{aligned}
\frac{\partial R_{\Gamma,i}(v,t \mid v_0)}{\partial t}+\frac{eE}{m_\Gamma^*}\frac{\partial R_{\Gamma,i}(v,t \mid v_0)}{\partial v} &= -\frac{1}{\tau_{\Gamma\Gamma}}[R_{\Gamma,i}(v,t \mid v_0)-R_{\Gamma,\mathrm{LE}}(v,t \mid v_0)] \\
&\quad -\frac{\Theta(v^2-v_c^2)}{\tau_{\Gamma L}}\left[R_{\Gamma,i}(v,t \mid v_0)-\frac{n_\Gamma^0 n_L(t)}{n_L^0 n_\Gamma(t)}R_{\Gamma,\mathrm{LE}}(v,t \mid v_0)\right], \\
\frac{\partial R_{L,i}(v,t \mid v_0)}{\partial t}+\frac{eE}{m_L^*}\frac{\partial R_{L,i}(v,t \mid v_0)}{\partial v} &= -\frac{1}{\tau_{LL}}[R_{L,i}(v,t \mid v_0)-R_{L,\mathrm{LE}}(v,t \mid v_0)] \\
&\quad -\frac{1}{\tau_{L\Gamma}}\left[R_{L,i}(v,t \mid v_0)-\frac{n_\Gamma^{\gtrless}(t)n_L^0}{n_\Gamma^{0,>}n_L(t)}R_{L,\mathrm{LE}}(v,t \mid v_0)\right],
\end{aligned} \tag{A1}$$

with $\tau_{\Gamma L}/\tau_{L\Gamma}=n_\Gamma^{0,>}/n_L^0$. The subscript i can be either Γ or L depending on which of the two sets of initial conditions is used

$$\begin{aligned}
&R_{\Gamma,\Gamma}(v,t=0 \mid v_0)=\delta(v-v_0), \quad i=\Gamma \text{ (starts in the } \Gamma \text{ valley)}, \\
&R_{L,\Gamma}(v,t=0 \mid v_0)=0, \quad i=\Gamma \text{ (starts in the } \Gamma \text{ valley)},
\end{aligned} \tag{A2}$$

or

$$\begin{aligned}
&R_{\Gamma,L}(v,t=0 \mid v_0)=0, \quad i=L \text{ (starts in the } L \text{ valley)}, \\
&R_{L,L}(v,t=0 \mid v_0)=\delta(v-v_0), \quad i=L \text{ (starts in the } L \text{ valley)}.
\end{aligned} \tag{A3}$$

$R_{\Gamma,\mathrm{LE}}(v,t \mid v_0)$ is the local-equilibrium function for the function R. This is just a Maxwellian (with the appropriate mass) that is normalized to the time-dependent density of the given valley, i.e.,

$$R_{\Gamma,\mathrm{LE}}(v,t \mid v_0)=\frac{\exp\left[\dfrac{-m_\Gamma^* v^2}{2k_B T_0}\right]}{(2\pi k_B T_0/m_\Gamma^*)^{1/2}}\int_{-\infty}^{\infty} dv' R_{\Gamma,i}(v',t \mid v_0). \tag{A4}$$

The analogous quantity is also defined for the L valley.

In these equations, n_L and n_Γ, etc., are now the probability of finding the initial electron in the Γ or L valley (i.e., the integral over the appropriate R) and depend on time (as well as the initial conditions). Care should be used in distinguishing them from the quantities that appear in the equations for the f's (where the normalization is slightly different—the f's are normalized to the total density n_{tot} while the R's are normalized to 1 since they are for a single electron).

To solve these equations, we first Laplace-transform them:

$$s\tilde{R}_{\Gamma,i}(v,s \mid v_0)+\frac{eE}{m_\Gamma^*}\frac{\partial\tilde{R}_{\Gamma,i}(v,s \mid v_0)}{\partial v}=-\frac{1}{\tau_{\Gamma\Gamma}}[\tilde{R}_{\Gamma,i}(v,s \mid v_0)-\tilde{R}_{\Gamma,\mathrm{LE}}(v,t \mid v_0)]$$
$$-\frac{\Theta(v^2-v_c^2)}{\tau_{\Gamma L}}\left[\tilde{R}_{\Gamma,i}(v,s \mid v_0)-\frac{n_\Gamma^0\tilde{n}_L(s)}{n_L^0\tilde{n}_\Gamma(s)}\tilde{R}_{\Gamma,\mathrm{LE}}(v,t \mid v_0)\right]+R_{\Gamma,i}(v,t=0 \mid v_0)\ , \tag{A5}$$

$$s\tilde{R}_{L,i}(v,s \mid v_0)+\frac{eE}{m_L^*}\frac{\partial\tilde{R}_{L,i}(v,s \mid v_0)}{\partial v}=-\frac{1}{\tau_{LL}}[\tilde{R}_{L,i}(v,s \mid v_0)-\tilde{R}_{L,\mathrm{LE}}(v,t \mid v_0)]$$
$$-\frac{1}{\tau_{L\Gamma}}\left[\tilde{R}_{L,i}(v,s \mid v_0)-\frac{\tilde{n}^{>}_{\Gamma}(s)n_L^0}{n_\Gamma^{0,>}\tilde{n}_L(s)}\tilde{R}_{L,\mathrm{LE}}(v,t \mid v_0)\right]+R_{L,i}(v,t=0 \mid v_0)\ .$$

Instead of solving for the full frequency dependence of the quantities, we will solve for only the low-frequency quantities since this simplifies the problem. The procedure to solve for the fully frequency-dependent quantities is similar but more complicated.

We expand the response functions in powers of s, the Laplace-transform variable

$$\tilde{R}_{\Gamma,i}(v,s \mid v_0)=\frac{\tilde{R}^{\,0}_{\Gamma,i}(v \mid v_0)}{s}+\tilde{R}^{\,1}_{\Gamma,i}(v \mid v_0)+s\tilde{R}^{\,2}_{\Gamma,i}(v \mid v_0)+\cdots\ ,$$
$$\tilde{R}_{L,i}(v,s \mid v_0)=\frac{\tilde{R}^{\,0}_{L,i}(v \mid v_0)}{s}+\tilde{R}^{\,1}_{L,i}(v \mid v_0)+s\tilde{R}^{\,2}_{L,i}(v \mid v_0)+\cdots\ . \tag{A6}$$

From the property of Laplace transforms, we know that $\lim_{s\to 0}s\tilde{R}_{\Gamma,i}(v,s \mid v_0)=\lim_{t\to\infty}R_{\Gamma,i}(v,t \mid v_0)$. Since as $t\to\infty$, the response function goes to the steady-state distribution function (normalized to 1) independent of initial conditions, we see that

$$\tilde{R}^{\,0}_{\Gamma,i}(v \mid v_0)=\frac{f_\Gamma(v)}{n_{\mathrm{tot}}}\ ,$$
$$\tilde{R}^{\,0}_{L,i}(v \mid v_0)=\frac{f_L(v)}{n_{\mathrm{tot}}}\ . \tag{A7}$$

If we substitute Eq. (A6) into Eq. (A5) and collect terms to linear order in s, we obtain the following pair of equations:

$$\frac{f_\Gamma(v)}{n_{\mathrm{tot}}}+\frac{eE}{m_\Gamma^*}\frac{\partial\tilde{R}^{\,1}_{\Gamma,i}(v \mid v_0)}{\partial v}=-\frac{1}{\tau_{\Gamma\Gamma}}\left[\tilde{R}^{\,1}_{\Gamma,i}(v \mid v_0)-\tilde{n}^{\,1}_{\Gamma}\frac{e^{-m_\Gamma^* v^2/2kT_0}}{(2\pi kT_0/m_\Gamma^*)^{1/2}}\right]$$
$$-\frac{\Theta(v^2-v_c^2)}{\tau_{\Gamma L}}\left[\tilde{R}^{\,1}_{\Gamma,i}(v \mid v_0)-\frac{n_\Gamma^0}{n_L^0}\tilde{n}^{\,1}_{L}\frac{e^{-m_\Gamma^* v^2/2kT_0}}{(2\pi kT_0/m_\Gamma^*)^{1/2}}\right]+R_{\Gamma,i}(v,t=0 \mid v_0)\ ,$$
$$\frac{f_L(v)}{n_{\mathrm{tot}}}+\frac{eE}{m_L^*}\frac{\partial\tilde{R}^{\,1}_{L,i}(v \mid v_0)}{\partial v}=-\frac{1}{\tau_{LL}}\left[\tilde{R}^{\,1}_{L,i}(v \mid v_0)-\tilde{n}^{\,1}_{L}\frac{e^{-m_L^* v^2/2kT_0}}{(2\pi kT_0/m_L^*)^{1/2}}\right] \tag{A8}$$
$$-\frac{1}{\tau_{L\Gamma}}\left[\tilde{R}^{\,1}_{L,i}(v \mid v_0)-\frac{n_L^0}{n_\Gamma^{0,>}}\tilde{n}^{\,>,1}_{\Gamma}\frac{e^{-m_L^* v^2/2kT_0}}{(2\pi kT_0/m_L^*)^{1/2}}+R_{L,i}(v,t=0 \mid v_0)\right]\ .$$

Here $\tilde{n}^{\,1}_{\Gamma}$ and $\tilde{n}^{\,1}_{L}$ are the integrals over v of $\tilde{R}^{\,1}_{\Gamma,i}(v \mid v_0)$ and $\tilde{R}^{\,1}_{L,i}(v \mid v_0)$, respectively, and $\tilde{n}^{\,>,1}_{\Gamma}$ is the integral over v of $\tilde{R}^{\,1}_{\Gamma,i}(v \mid v_0)$ for $|v|>v_c$. They are also the first terms in the expansion of the densities in the Laplace-transform variable s, i.e.,

$$\tilde{n}_\Gamma(s)=\frac{n_\Gamma}{s}+\tilde{n}^{\,1}_{\Gamma}(v_0)+s\tilde{n}^{\,2}_{\Gamma}(v_0)+\cdots\ ,$$
$$\tilde{n}_L(s)=\frac{n_L}{s}+\tilde{n}^{\,1}_{L}(v_0)+s\tilde{n}^{\,2}_{L}(v_0)+\cdots\ .$$

If the density in each valley is constant in time (does not fluctuate), then all higher-order terms vanish, i.e.,

$$\tilde{n}^{\,1}_{\Gamma}=\tilde{n}^{\,2}_{\Gamma}=\cdots=0\ ,$$
$$\tilde{n}^{\,1}_{L}=\tilde{n}^{\,2}_{L}=\cdots=0\ .$$

$\tilde{n}^{\,1}_{\Gamma}$ and $\tilde{n}^{\,1}_{L}$ are the (low-frequency) density response functions (for the given initial velocity v_0). Since the total density is a constant, $\tilde{n}_\Gamma+\tilde{n}_L=1/s$ and therefore

$$\tilde{n}^{\,1}_{\Gamma}=-\tilde{n}^{\,1}_{L},\quad \tilde{n}^{\,2}_{\Gamma}=-\tilde{n}^{\,2}_{L},\quad \ldots\ . \tag{A9}$$

Equations (A8) are a rather complicated set of equations, especially since the expressions for $f_\Gamma(v)$ and $f_L(v)$ are com-

plicated in themselves (see Ref. 7). In addition, the coupled pair of equations must be solved for both sets of initial conditions given by Eqs. (A2) and (A3). To solve the equations, one first integrates them using an integrating factor to find $\tilde{R}^{\,1}_{\Gamma,i}(v \mid v_0)$ and $\tilde{R}^{\,1}_{L,i}(v \mid v_0)$ as functionals of $\tilde{n}^{\,1}_{\Gamma}$, $\tilde{n}^{\,1}_{L}$, and $\tilde{n}^{\,>,1}_{\Gamma}$. The first is given by

$$\tilde{R}^{\,1}_{\Gamma,i}(v \mid v_0)=\int_{-\infty}^{v} dv' \frac{m^*_\Gamma}{eE}\exp\left[-\frac{m^*_\Gamma}{eE}\left[\frac{1}{\tau_{\Gamma\Gamma}}+\frac{1}{\tau_{\Gamma L}}\right](v-v')\right] \times\left[\left[\frac{\tilde{n}^{\,1}_{\Gamma}}{\tau_{\Gamma\Gamma}}+\frac{n^0_\Gamma}{n^0_L}\frac{\tilde{n}^{\,1}_{L}}{\tau_{\Gamma L}}\right]\frac{e^{-m^*_\Gamma v'^2/2kT_0}}{(2\pi kT_0/m^*_\Gamma)^{1/2}}+R_{\Gamma,i}(v',t=0 \mid v_0)-\frac{f_\Gamma(v')}{n_{\rm tot}}\right], \quad v<-v_c$$

$$\tilde{R}^{\,1}_{\Gamma,i}(v \mid v_0)=\exp\left[\frac{-m^*_\Gamma}{eE\tau_{\Gamma\Gamma}}(v+v_c)\right]\tilde{R}^{\,1}_{\Gamma,i}(-v_c \mid v_0)+\int_{-v_c}^{v} dv' \frac{m^*_\Gamma}{eE}\exp\left[\frac{-m^*_\Gamma}{eE\tau_{\Gamma\Gamma}}(v-v')\right] \times\left[\frac{\tilde{n}^{\,1}_{\Gamma}}{\tau_{\Gamma\Gamma}}\frac{e^{-m^*_\Gamma v'^2/2kT_0}}{(2\pi kT_0 m^*_\Gamma)^{1/2}}+R_{\Gamma,i}(v',t=0 \mid v_0)-\frac{f_\Gamma(v')}{n_{\rm tot}}\right], \quad -v_c<v<v_c \tag{A10}$$

$$\tilde{R}^{\,1}_{\Gamma,i}(v \mid v_0)=\exp\left[\frac{m^*_\Gamma}{eE}\left[\frac{1}{\tau_{\Gamma\Gamma}}+\frac{1}{\tau_{\Gamma L}}\right](v-v')\right]\tilde{R}^{\,1}_{\Gamma,i}(v_c \mid v_0)+\int_{v_c}^{v} dv' \frac{m^*_\Gamma}{eE}\exp\left[-\frac{m^*_\Gamma}{eE}\left[\frac{1}{\tau_{\Gamma\Gamma}}+\frac{1}{\tau_{\Gamma L}}\right](v-v')\right] \times\left[\left[\frac{\tilde{n}^{\,1}_{\Gamma}}{\tau_{\Gamma\Gamma}}+\frac{n^0_\Gamma}{n^0_L}\frac{\tilde{n}^{\,1}_{L}}{\tau_{\Gamma L}}\right]\frac{e^{-m^*_\Gamma v'^2/2kT_0}}{(2\pi kT_0/m^*_\Gamma)^{1/2}}+R_{\Gamma,i}(v',t=0 \mid v_0)-\frac{f_\Gamma(v')}{n_{\rm tot}}\right], \quad v_c<v$$

and the expression for $\tilde{R}^{\,1}_{L,i}(v \mid v_0)$ is given by

$$\tilde{R}^{\,1}_{L,i}(v \mid v_0)=\frac{m^*_L}{eE}\int_{-\infty}^{v} dv'\exp\left[\frac{-m^*_L}{eE}\left[\frac{1}{\tau_{LL}}+\frac{1}{\tau_{L\Gamma}}\right](v-v')\right] \times\left[\left[\frac{\tilde{n}^{\,1}_{L}}{\tau_{LL}}+\frac{n^0_L}{n^{0,>}_\Gamma}\frac{\tilde{n}^{\,1}_{\Gamma}}{\tau_{L\Gamma}}\right]\frac{e^{-m^*_L v'^2/2kT_0}}{(2\pi kT_0/m^*_L)^{1/2}}+R_{L,i}(v',t=0 \mid v_0)-\frac{f_L(v')}{n_{\rm tot}}\right]. \tag{A11}$$

These equations are rather horrifying, especially since the expressions for $f_\Gamma(v)$ and $f_L(v)$ still must be substituted into them and one still has to determine the density by integrating over $\tilde{R}^{\,1}_{\Gamma,i}(v \mid v_0)$. Nevertheless, these equations represent the solution to the coupled equations (A8) once the quantities $\tilde{n}^{\,1}_{\Gamma}$, $\tilde{n}^{\,1}_{L}$, and $\tilde{n}^{\,>,1}_{\Gamma}$ are determined.

Determining the densities. To determine the self-consistent densities, $\tilde{n}^{\,1}_{\Gamma}$, $\tilde{n}^{1}_{L}$, and $\tilde{n}^{\,>,1}_{\Gamma}$, it is necessary to have three equations relating these densities. The first relation is Eq. (A9) and is a result of the fact that the total density is constant. The second is obtained by integrating either one of the Eqs. (A8) over v from $-\infty$ to ∞ and is given by

$$n_L=-\frac{1}{\tau_{L\Gamma}}\left[\tilde{n}^{\,1}_{L}-\frac{n^0_L}{n^{0,>}_\Gamma}\tilde{n}^{\,>,1}_{\Gamma}\right]+n_L(t=0) . \tag{A12}$$

The third equation is obtained by integrating the first of Eqs. (A8) from $-v_c$ to v_c to obtain

$$n_\Gamma-n^{\,>}_{\Gamma}+\frac{eE}{m^*_\Gamma}[\tilde{R}^{\,1}_{\Gamma,i}(v_c \mid v_0)-\tilde{R}^{\,1}_{\Gamma,i}(-v_c \mid v_0)] =-\frac{1}{\tau_{\Gamma\Gamma}}(\alpha\tilde{n}^{\,1}_{\Gamma}-\tilde{n}^{\,>,1}_{\Gamma})+\int_{-v_c}^{v_c} dv' R_{\Gamma,i}(v',t=0 \mid v_0) . \tag{A13}$$

Here, $\alpha=\mathrm{erfc}[(\Delta/k_BT_0)^{1/2}]$ is the fraction of electrons in the Γ valley with energies above Δ in equilibrium.

There are two cases, corresponding to which valley the electron starts out in. In both cases, since $\tilde{R}^{\,1}_{\Gamma,i}(v_c \mid v_0)$ is a linear function of $\tilde{n}^{\,1}_{\Gamma}$, $\tilde{n}^{\,1}_{L}$, and $\tilde{n}^{\,>,1}_{\Gamma}$, we have three linear equations in three unknowns. These equations can be solved in each case. In the case that the electron starts out in the L valley, we find that the expressions do not depend on what the initial velocity is, but if the electron starts out in the Γ valley then the densities have a dependence on the initial velocity v_0. This is not surprising. If an electron is in the L valley, then it always has enough energy to transfer to the Γ valley. However, an electron in the Γ valley must have an energy above Δ to transfer to the L valley and thus the expressions for the densities have a dependence on the initial value of the velocity v_0.

Starting in the L valley. The expressions for the densities when the electron starts out in the L valley are obtained by solving the linear system of three equations and are given by

$$\tilde{n}^{\,1}_{\Gamma}=(B_1+E_1)/(A_1+D_1) , \tag{A14}$$

$$\tilde{n}^{\,1}_{L}=-\tilde{n}^{\,1}_{\Gamma} , \tag{A15}$$

$$\tilde{n}^{\,>,1}_{\Gamma}=-B_1+A_1(\tilde{n}^{\,1}_{\Gamma}) . \tag{A16}$$

Here A_1, B_1, D_1, and E_1 are constants (they depend only on the electric field):

$$A_1=\left[\exp\left[-\frac{m^*_\Gamma 2v_c}{eE\tau_{\Gamma\Gamma}}\right]-1\right]a_1+e_1+\frac{\alpha}{\tau_{\Gamma\Gamma}} , \tag{A17}$$

$$B_1=\left[1-\exp\left[\frac{-m^*_\Gamma 2v_c}{eE\tau_{\Gamma\Gamma}}\right]\right]b_1-d_1-f_1+n^{\,>}_{\Gamma}-n_\Gamma , \tag{A18}$$

$$D_1=\frac{n_\Gamma^0}{n_L^0}\frac{\alpha}{\tau_{\Gamma\Gamma}}\ , \tag{A19}$$

$$E_1=-n_\Gamma\frac{\tau_{\Gamma L}}{\tau_{\Gamma\Gamma}}\ . \tag{A20}$$

The expressions for a_1, b_1, d_1, e_1, and f_1 are

$$a_1=\left[\frac{1}{\tau_{\Gamma\Gamma}}-\frac{n_\Gamma^0}{n_L^0}\frac{1}{\tau_{\Gamma L}}\right]\times\int_{-\infty}^{-v_c}dv'\exp\left[\frac{m_\Gamma^*}{eE}\left[\frac{1}{\tau_{\Gamma\Gamma}}+\frac{1}{\tau_{\Gamma L}}\right](v_c+v')\right]\times\frac{e^{-m_\Gamma^* v'^2/2kT_0}}{(2\pi kT_0/m_\Gamma^*)^{1/2}}\ ,$$

$$b_1=\frac{m_\Gamma^*}{eE}\left[\frac{n_\Gamma}{\tau_{\Gamma\Gamma}}+\frac{n_\Gamma^0}{n_L^0}\frac{n_L}{\tau_{\Gamma L}}\right]\times\int_{-\infty}^{-v_c}dv'\exp\left[\frac{m_\Gamma^*}{eE}\left[\frac{1}{\tau_{\Gamma\Gamma}}+\frac{1}{\tau_{\Gamma L}}\right](v_c+v')\right]\times(v_c+v')\frac{e^{-m_\Gamma^* v'^2/2kT_0}}{(2\pi kT_0/m_\Gamma^*)^{1/2}}\ ,$$

$$d_1=-2v_c\exp\left[\frac{m_\Gamma^*2v_c}{eE\tau_{\Gamma\Gamma}}\right]f_\Gamma(-v_c)\ , \tag{A21}$$

$$e_1=\int_{-v_c}^{v_c}dv'\frac{1}{\tau_{\Gamma\Gamma}}\exp\left[\frac{-m_\Gamma^*(v_c-v')}{eE\tau_{\Gamma\Gamma}}\right]\frac{e^{-m_\Gamma^* v'^2/2kT_0}}{(2\pi kT_0/m_\Gamma^*)^{1/2}}\ ,$$

$$f_1=\int_{-v_c}^{v_c}dv'\exp\left[\frac{-m_\Gamma^*(v_c-v')}{eE\tau_{\Gamma\Gamma}}\right]\times\frac{n_\Gamma m_\Gamma^*(v_c-v')}{eE\tau_{\Gamma\Gamma}}\frac{e^{-m_\Gamma^* v'^2 2kT_0}}{(2\pi kT_0/m_\Gamma^*)^{1/2}}\ .$$

Most of these integrals can be evaluated analytically in terms of error functions.

Starting in the Γ valley. For the case that the electron starts out in the Γ valley, the expressions for $\tilde{n}_\Gamma^{\downarrow}$, $\tilde{n}_L^{\downarrow}$, and $\tilde{n}_\Gamma^{\rightarrow,\downarrow}$ are given by the above expressions with A_1 and D_1 given by Eqs. (A17) and (A19) but with B_1 and E_1 now given by

$$B_1=\left[1-\exp\left[\frac{-m_\Gamma^*2v_c}{eE\tau_{\Gamma\Gamma}}\right]\right](b_1+c_1)-d_1-f_1-g_1+n_\Gamma^{\rightarrow}-n_\Gamma-\Theta(v_c-v)\Theta(v+v_c)\ , \tag{A22}$$

$$E_1=(1-n_\Gamma)\frac{\tau_{\Gamma L}}{\tau_{\Gamma\Gamma}}\ . \tag{A23}$$

The expressions for a_1, b_1, d_1, e_1, and f_1 are the same as before, and the expressions for c_1 and g_1 are given by

$$c_1(v_0)=\Theta(-v_c-v_0)\times\exp\left[\frac{m_\Gamma^*}{eE}\left[\frac{1}{\tau_{\Gamma\Gamma}}+\frac{1}{\tau_{\Gamma L}}\right](v_c+v_0)\right]\ , \tag{A24}$$

$$g_1(v_0)=\Theta(v_c-v_0)\Theta(v_0+v_c)\times\exp\left[\frac{-m_\Gamma^*(v_c-v_0)}{eE\tau_{\Gamma\Gamma}}\right]\ . \tag{A25}$$

Note that B_1 no longer is a constant but has a dependence on the initial velocity both through expressions for c_1 and g_1 and the last term in Eq. (A22). These equations solve the equation for the Green functions. To determine the current fluctuations, we still have to integrate over the Green functions and the steady state distribution functions.

Expressions for the power spectra. Rather than directly integrate over the Green functions to obtain the expression for the power spectra, some simplification is made if the equations for the Green functions are directly multiplied by v and v_0 and the appropriate steady-state distribution function [either $f_\Gamma(v_0)$ or $f_L(v_0)$], then integrated over v and v_0. We find four contributions to the noise spectra, denoted by $S_{\Gamma,\Gamma}$, $S_{L,L}$, $S_{\Gamma,L}$, $S_{L,L}$ and given by

$$S_{L,L}(\omega=0,E)=\frac{A}{2l}\left[\frac{4n_L e^2 k_B T_0/m_L^*}{\frac{1}{\tau_{LL}}+\frac{1}{\tau_{L\Gamma}}}+\frac{4I_L^2(2-n_L)/n_L}{\frac{1}{\tau_{LL}}+\frac{1}{\tau_{L\Gamma}}}+4I_L^2\frac{\tilde{n}_L^{\downarrow}}{n_L}\right]\ , \tag{A26}$$

$$S_{\Gamma,L}(\omega=0,E)=\frac{A}{2l}\left[\frac{-4I_L I_\Gamma}{\frac{1}{\tau_{LL}}+\frac{1}{\tau_{L\Gamma}}}+\frac{4eI_L}{n_L}\int_{-\infty}^{\infty}dv_0 v_0\tilde{n}_L^{\downarrow}(v_0)f_\Gamma(v_0)\right]\ , \tag{A27}$$

$$S_{\Gamma,\Gamma}(\omega=0,E)=\frac{A}{2l}\left[4e^2\int_{-\infty}^{\infty}dv_0\frac{v_0^2 f_\Gamma(v_0)}{\frac{1}{\tau_{\Gamma\Gamma}}+\frac{\Theta(v_0^2-v_c^2)}{\tau_{\Gamma L}}}-4I_\Gamma^2\left[\tau_{\Gamma\Gamma}+\frac{1}{\frac{1}{\tau_{\Gamma\Gamma}}+\frac{1}{\tau_{\Gamma L}}}\right]+4\frac{e^2E}{m_\Gamma^*}I_\Gamma\frac{n_\Gamma\tau_{\Gamma\Gamma}}{\frac{1}{\tau_{\Gamma\Gamma}}+\frac{1}{\tau_{\Gamma L}}}+4\frac{e^2E}{m_\Gamma^*}\int_{-\infty}^{\infty}dv_0 v_0 f_\Gamma(v_0)\left[\tilde{n}_\Gamma^{\downarrow}(v_0)\tau_{\Gamma\Gamma}-\frac{\frac{\tau_{\Gamma\Gamma}}{\tau_{\Gamma L}}}{\frac{1}{\tau_{\Gamma\Gamma}}+\frac{1}{\tau_{\Gamma L}}}\times\{\tilde{n}_\Gamma^{\rightarrow,\downarrow}(v_0)+v_c[\tilde{R}_{\Gamma,\Gamma}^{\downarrow}(v_c\mid v_0)+\tilde{R}_{\Gamma,\Gamma}^{\downarrow}(-v_c\mid v_0)]\}\right]\right]\ , \tag{A28}$$

$$S_{L,\Gamma}(\omega=0,E)=\frac{A}{2l}\left\{4I_L\left[-I_\Gamma\left[\tau_{\Gamma\Gamma}+\frac{1}{\frac{1}{\tau_{\Gamma\Gamma}}+\frac{1}{\tau_{\Gamma L}}}\right.\right.\right.$$

$$\left.\left.\left.+\frac{e^2E}{m^*_\Gamma}\left[\frac{n_\Gamma\tau_{\Gamma\Gamma}}{\frac{1}{\tau_{\Gamma\Gamma}}+\frac{1}{\tau_{\Gamma L}}}-\tilde{n}^{\,1}_{\Gamma}\tau_{\Gamma\Gamma}-\frac{\frac{\tau_{\Gamma\Gamma}}{\tau_{\Gamma L}}}{\frac{1}{\tau_{\Gamma\Gamma}}+\frac{1}{\tau_{\Gamma L}}}\{\tilde{n}\,\tilde{\mathcal{E}}^{\,-1}+v_c[\tilde{R}^{\,1}_{\Gamma,L}(v_c)+\tilde{R}^{\,1}_{\Gamma,L}(-v_c)]\}\right]\right]\right\}, \tag{A29}$$

where A is the cross-sectional area and $2l$ the length of the sample.

The dominant contribution (cf. Fig. 2) is from $S_{\Gamma,\Gamma}$. One can divide $S_{\Gamma,\Gamma}$ up into the three expressions. The first expression (cf. solid line in Fig. 3) comes from dividing the first integral in (A28) into two pieces [by dividing $f_\Gamma(v_0)$ through the time-independent version of Eq. (1a)]; one an equilibrium piece proportional to $f_{\Gamma,\mathrm{eq}}$; the other a nonequilibrium piece proportional to $\partial f_\Gamma/\partial v$. The first expression in Fig. 3 (solid line) is this equilibrium piece. The second expression in Fig. 3 (short-dashed line) is the remaining nonequilibrium piece plus the next two terms in (A28) that are proportional to I_Γ^2 and I_Γ. The third and final expression (cf. long-dashed line in Fig. 6) is the remaining integral in (A28) (note that all the terms in this remaining integral are proportional to $\tilde{n}^{\,1}_{\Gamma}$ or $\tilde{n}\,\tilde{\mathcal{E}}^{\,-1}$ so that the third expression would equal zero in a one-valley model).

One word of caution should be said about the expressions for $S_{\Gamma,L}$ and $S_{L,\Gamma}$. The individual expressions have no physical meaning by themselves. The only quantity that should have any physical meaning is $\frac{1}{2}(S_{\Gamma,L}+S_{L,\Gamma})$. This is because in analytically continuing the Laplace expressions for $S_{\Gamma,L}(s)$ and $S_{L,\Gamma}(s)$ into frequency space, we have assumed that the individual correlation functions $\Gamma_{\Gamma,L}(t)$ and $\Gamma_{L,\Gamma}(t)$ are even functions of time. This is not necessarily true since stationarity only guarantees that the sum $\Gamma_{\Gamma,L}(t)+\Gamma_{L,\Gamma}(t)$ is even in time and thus the analytic continuation procedure is valid only for the sum of the two terms and not for the individual terms.

The expressions for $S_{L,L}$ and $S_{L,\Gamma}$ are easily evaluated in terms of the given expressions for the Green functions and the densities $\tilde{n}^{\,1}_{\Gamma}$, $\tilde{n}^{\,1}_{L}$, and $\tilde{n}\,\tilde{\mathcal{E}}^{\,-1}$. The expressions for $S_{\Gamma,\Gamma}$ and $S_{\Gamma,L}$ are more complicated since when the electron starts in the Γ valley, the expressions for the $\tilde{n}^{\,1}_{\Gamma}$, etc. depend on the initial velocity v_0, and this leads to terms that contain integrals over the initial conditions.

*Present address: Coordinated Science Laboratory, University of Illinois, Urbana, Illinois 61801.

[1]W. Fawcett and H. D. Rees, Phys. Lett. **29A**, 578 (1969).

[2]J. Požela and A. Reklaitis, Solid State Commun. **27**, 1073 (1978).

[3]T. H. Glisson, R. A. Sadler, J. R. Hauser, and M. A. Littlejohn, Solid-State Electron. **23**, 627 (1980).

[4]M. Abe, S. Yanagisawa, O. Wada, and H. Takanashi, Appl. Phys. Lett. **25**, 674 (1974).

[5]A. Chatterjee and P. Das, in *Noise in Physical Systems and 1/f Noise*, edited by M. Savelli, G. Lecoy, and J. P. Nougier (North-Holland, Amsterdam, 1983), pp. 161–164.

[6]P. N. Butcher, W. Fawcett, and N. R. Ogg, Brit. J. Appl. Phys. **18**, 755 (1967).

[7]Christopher J. Stanton, Harold U. Baranger, and John W. Wilkins, Appl. Phys. Lett. **49**, 176 (1986).

[8]W. Fawcett, in *Proceedings of the Tenth International Conference on the Physics of Semiconductors*, edited by S. P. Keller, J. C. Hensel, and F. Stern (National Technical Information Service, Oak Ridge, 1970), pp. 51–59.

[9]J. Pozhela and A. Reklaitis, Solid-State Electron. **23**, 927 (1980).

[10]J. G. Ruch and G. S. Kino, Phys. Rev. **174**, 921 (1968).

[11]D. Gasquet, M. de Murcia, J. P. Nougier, and C. Gontrand, Physica **134B**, 264 (1985).

[12]V. Bareikis, V. Viktoravichyus, A. Gal'dikas, and R. Milyushite, Fiz. Tekh. Poluprovodn. **14**, 1427 (1980) [Sov. Phys.—Semicond. **14**, 847 (1980)].

[13]D. E. Aspnes, Phys. Rev. B **14**, 5331 (1976).

[14]K. Brennan and K. Hess, Solid-State Electron. **27**, 347 (1984).

[15]Christopher J. Stanton, Ph.D. thesis, Cornell University, 1986 (unpublished).

[16]H. U. Baranger, Ph.D. thesis, Cornell University (University Microfilms International, Ann Arbor), 1986.

[17]Christopher J. Stanton and John W. Wilkins, Physica **134B**, 255 (1985).

[18]Christopher J. Stanton and John W. Wilkins, Phys. Rev. B **35**, 9722 (1987). See also Ref. 15.